ELSEVIER

Automation in Construction 11 (2002) 655–665

AUTOMATION IN CONSTRUCTION

www.elsevier.com/locate/autcon

Positional control of pneumatic manipulators for construction tasks

M.Yu. Rachkov, M. Crisóstomo, L. Marques, A.T. de Almeida*

Institute of Systems and Robotics, Department of Electrical and Computer Engineering, University of Coimbra, 3030-290 Coimbra, Portugal

Accepted 1 February 2002

Abstract

This paper describes solutions that can be applied to pneumatic manipulator problems in positioning, both for angle trajectories and for long linear trajectories, used in construction tasks. Optimal positioning of a pneumatic manipulator along angle trajectories with minimum control energy consumption is given. The implementation of the control system is presented. Control algorithms for a long linear trajectory manipulator based on two-phase and three-phase motion modes of the end-effector are investigated. Conventional and fuzzy logic controls of a pneumatic manipulator were applied and experimental testing was carried out. The obtained results allow widening the application range of pneumatic manipulators in construction, particularly in gantry type machines.

Keywords: Pneumatic manipulators; Positional accuracy; Control optimization

1. Introduction

The advantages of pneumatic manipulators for construction applications are high speed and force capabilities coupled with smaller sizes, compared to electricity-driven manipulators. Pneumatic manipulators have a high payload-to-weight ratio that is especially important for their usage with wall-climbing robots to fulfill different construction operations [1,2]. An essential application limitation of conventional industrial pneumatic manipulators is an impossibility to change a given program for the end-effector trajectories during motion.

A hierarchical feedback control for pneumatic manipulators was proposed in Ref. [3]. However, it is difficult to compensate payload and supply pressure variation in such a way. A pneumatic manipulator control based on recursive identification is described inRef. [4]. A stability of this controlled motion is not guaranteed. It was concluded in Ref. [5] that third-order control provides a practical choice for effective control of industrial pneumatic manipulators. Sometimes, in practice, it is necessary to have minimum control energy consumption for autonomous manipulators. The problem of optimal control is important in this case [6].

The considered problem of a flexible positioning system design is solved for a widespread type of industrial robots with an angle manipulator drive consisting of two double-acting pneumatic power cylinders.

Some building inspection operations require working in long linear trajectories with good position accuracy. This may be carried out by means of long cylinders with appropriate monitoring equipment connected to the end-effector. The main difficulties in this case are to combine velocity during the motion with high accuracy at the desired positioning.

* Corresponding author. Tel.: +351-239-796-218; fax: +351-239-406-672.

E-mail address: adealmeida@isr.uc.pt (A.T. de Almeida).

0926-5805/02/$ - see front matter
PII: S0926-5805(02)00007-9

The above-mentioned problems of pneumatic manipulators positioning for construction applications are addressed in this paper.

2. Positioning of a pneumatic manipulator in angle trajectories

2.1. Description of the system

A diagram of the manipulator drive is presented in Fig. 1.

The manipulator 1 of a length L and a gripper with an object 2 of mass m, is actuated by double-acting pneumatic power cylinder 3 through a gear 4 with a lever l. The considered drive system with pressure variation in pneumatic power cylinders [7] is described by non-linear differential equations of the third order

$$\ddot{\varphi} = p\frac{2F_{\mathrm{n}}l}{mL^2} - f(\dot{\varphi})$$

$$\dot{p} = -\frac{2PF_{\mathrm{n}}l}{V}\dot{\varphi} + \frac{RT}{V}g; \qquad (2.1.1)$$

where φ is angular position of the manipulator gripper, p is current pressure difference in pneumatic cylinder volumes, F_{n} is square of the cylinder piston, l is lever of acting force, R is gas constant, T is absolute temperature of working gas, V is full volume of the pneumatic cylinder, P is pressure in the volumes of the cylinder in an equilibrium position of a cylinder piston, g is molar gas consumption in pneumatic cylinder volumes, $f(\dot{\varphi})$ is summand taking into account a friction force of the drive system. The force of inertia for rather large values of mass m considerably exceeds friction force in the drive system. In this case, it is possible to transform a system (Eq. (2.1.1)) as follows

$$\dot{x}_1 = a_{13}x_3$$

$$\dot{x}_2 = x_1$$

$$\dot{x}_3 = -a_{31}x_1 + u; \qquad (2.1.2)$$

where

$$x_1 = \dot{\varphi},\ x_2 = \varphi,\ x_3 = p,$$

$$a_{13} = \frac{2F_{\mathrm{n}}l}{mL^2},\ a_{31} = \frac{2PF_{\mathrm{n}}l}{V},\ u = \frac{RT}{V}g. \qquad (2.1.3)$$

Thus, phase coordinates of the system are an angular position and angular velocity of the manipulator gripper and pressure in pneumatic power cylinders. A control parameter is the gas consumption.

A problem of minimization of positioning coordinates of the system (2.1.2) and simultaneously of control energy consumptions should be solved. It is possible to solve the optimal control task by means of the following quadratic functional

$$I = \int_0^{\infty} (r_2x_2^2 + r_3x_3^2 + \rho u^2)\mathrm{d}t, \qquad (2.1.4)$$

where $x_2 = \varphi$, $x_3 = p$, $u = ((RT)/V)g$, and r_2, r_3, ρ—coefficients depending on a construction task. The control of the system carries out by means of a gas consumption valve. Information about a current system state is obtained from a sensor block.

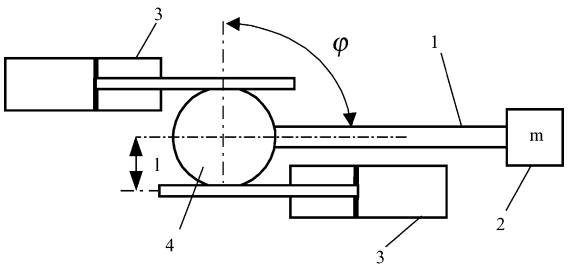

Fig. 1. Diagram of the manipulator drive.

2.2. Synthesis of the control system

For the considered stationary system we can use an equation [8]:

$$R_1 - P\mathbf{B}R_2^{-1}\mathbf{B}'P + \mathbf{A}P + P\mathbf{A} = 0, \qquad (2.2.1)$$

where the matrices $\mathbf{A}$ and $\boldsymbol{B}$ are determined according to Ref. [7], and

$$R_1 = \begin{bmatrix} 0 & 0 & 0 \\ 0 & r_2 & 0 \\ 0 & 0 & r_3 \end{bmatrix}; \quad R_2 = \rho;$$

$$P = \begin{bmatrix} P_{11} & P_{12} & P_{13} \\ P_{21} & P_{22} & P_{23} \\ P_{31} & P_{32} & P_{33} \end{bmatrix}. \qquad (2.2.2)$$

An optimal control of the system (2.1.2), Eq. (2.1.4) can be written as follows

$$u_o = -R_2^{-1}\mathbf{B}'\,PX = -\rho^{-1}(P_{31}x_1 + P_{32}x_2 + P_{33}x_3), \qquad (2.2.3)$$

where the elements $i = 1, 2, 3$ are amplifying coefficients in the feedback loop of the control system.

The problem of the optimal control is reduced to a determination of necessary elements of the matrix **P**, which can be obtained from Eq. (2.2.1). For such a purpose a solution algorithm of the Eq. (2.2.1) for stationary systems with infinite time of observation [8] can be used. Necessary elements of the matrix **P** can be defined according to Ref. [9]. Using them in Eq. (2.2.3), we obtain the optimal control.

The system by the obtained optimal control is asymptotically stable. Experimental results with a manipulator of the robot "Tsiclon" [7] show that all disturbances are tended to zero exponential quickly. Response time is inside 2 s for the 180° control angle range.

An implementation of the optimal control (Eq. (2.2.3)) with a simulation of the object (Eq. (2.1.2)) is shown in Fig. 2.

Thus, the implementation of the optimal control demands only three scaling blocks and one summator. The control signal is used in the drive for the optimal positioning of the manipulator.

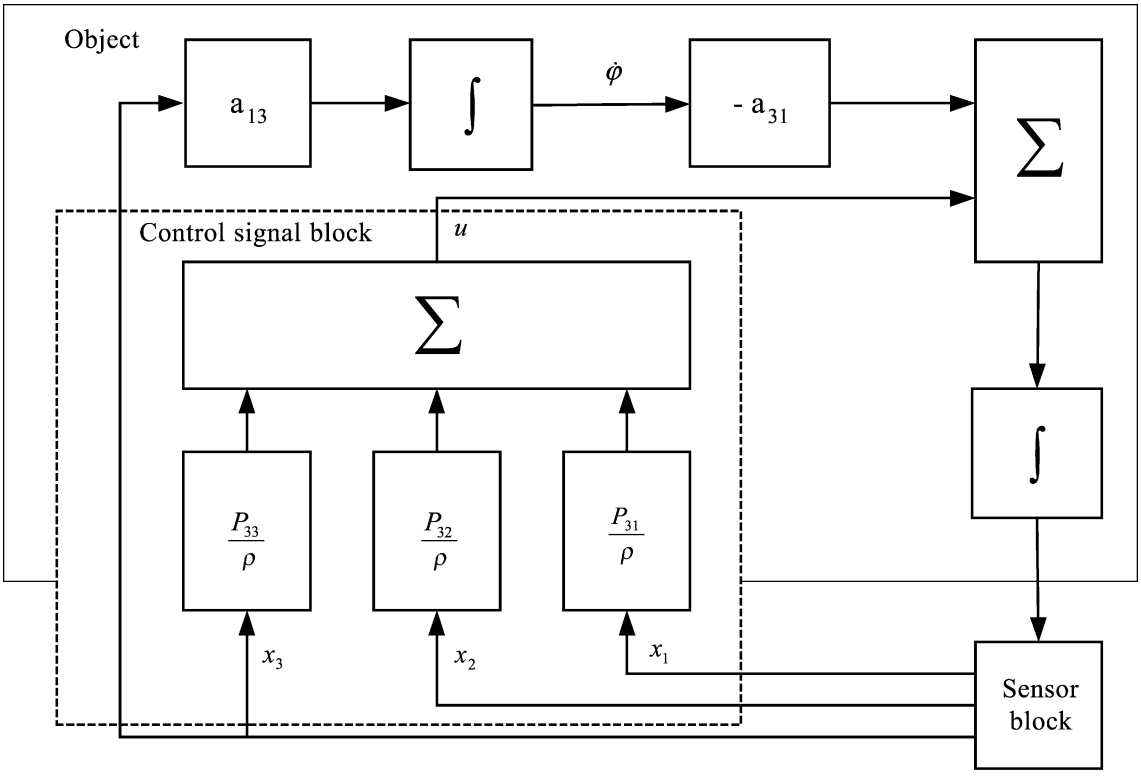

Fig. 2. Implementation of the optimal control.

The presented accounting algorithm for the control system can be used for any type of manipulators that are actuated by means of two double-acting pneumatic power cylinders.

3. Positioning of a pneumatic manipulator in long linear trajectories

3.1. Description of the system

Some building inspection operations require working along long linear trajectories with good positional accuracy. This may be carried out by means of long cylinders with necessary technological equipment connected to the end-effector. The main difficulties in this case are to combine velocity during the motion with high accuracy at the desired positioning. A rodless pneumatic manipulator can be applied to fulfill the described task. A diagram of the manipulator is shown in Fig. 3.

The manipulator has a rodless pneumatic cylinder with the piston connected to the tool of the mass M to be moved. The tool position is measured by an incremental optical encoder. A current-commanded proportional valve controls the airflow in the cylinder chambers. The control algorithm is run by means of a microcontroller that interfaces to the encoder and to the valve through a 12-bit digital-to-analog converter (DAC). A PC connected by an RS232 serial interface to the controller monitors the system.

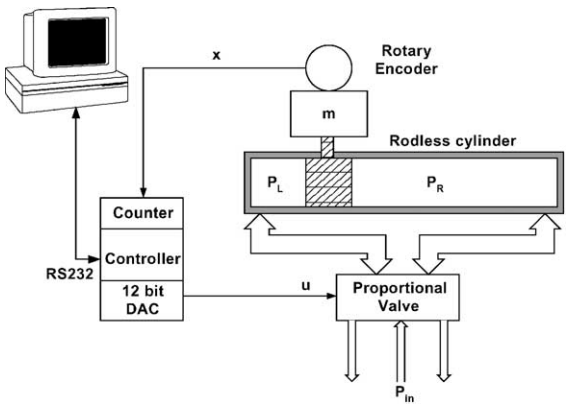

Fig. 3. Diagram of the linear pneumatic manipulator.

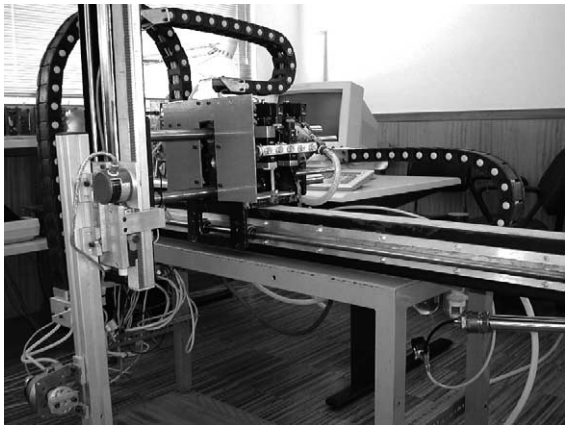

Fig. 4. General view of the long linear trajectory manipulator.

The general view of the system is shown in Fig. 4.

The system has 5 *df*. There are 3 *df* related to transporting motion (x, y, z), rotation motion of the gripper, and gripping motion. X-motion is performed by a linear stage composed by an Origa P210 rodless cylinder with 1200-mm stroke and 25-mm piston diameter. The payload moved by this cylinder is 46 kg and the medium static friction is 3.5 kgf. The end-effector position is measured with 20 μm accuracy by a rotary incremental encoder toothed to the fixed structure. The airflow is controlled by a proportional valve. The current through the valve solenoid defines five working zones: from 0 to 300 mA the valve is completely open in one direction (say A); from 300 to 500 mA the flow in direction A changes linearly; from 500 to 600 mA the valve is closed; from 600 to 800 mA the flow changes linearly in the other direction (say B); above 800 mA the valve is completely open in direction B. The valve electrical current is controlled with 12-bit accuracy DAC. The working pressure is 6 bar and the connecting nylon tubes of 4-mm interior diameter. In order to deal with the solenoid hysteresis, the command current is summed with a 50-Hz sinusoidal current. In order to not disturb the system, the frequency of the summed signal was chosen much higher then the frequency of the system (less then 2 Hz depending on the command amplitude).

The dynamics of pressure P_i in the i-th chamber can be described by the following equation

$$\dot{P}_i = \frac{f_i}{x} S_i - k \frac{P_i}{x} \dot{x},$$

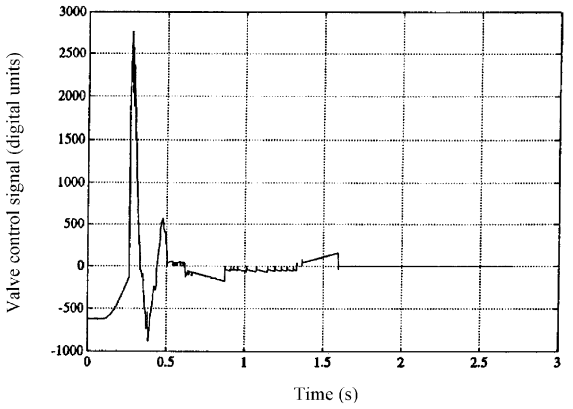

Fig. 5. Command signal versus time in seconds.

where S_i is the valve cross-sectional area, k is the ratio of specific heats, x is the piston position,

$$f_i = \frac{kT_i}{A_i}\sqrt{\frac{2R}{T_i}}P_u Y\left(\frac{P_d}{P_u}\right),$$

where T_i is absolute temperature, R is the universal gas constant, P_u and P_d are upper and lower pressures correspondingly and Y is a constant coefficient [10],

$$S_i \cong k_v u_i,$$

where k_v is the valve proportional constant and u_i is the valve input signal.

The system dynamics can be modeled by the following equation

$$M\ddot{x} + B\dot{x} + L = A(P_L - P_R),$$

where M represents the moving mass, B is the viscous-damping coefficient, L represents disturbances because of static and Coulomb friction, A is the piston area and P_L and P_R are the pressures in left and right chambers correspondingly.

Experimental research of the rodless pneumatic manipulator shows that friction has essential influence on a control algorithm of this system. From the other side, friction has a stochastic character sometimes. In this case, one of the most reliable solutions to control the system is an experimental approach.

3.2. Experimental optimization

To achieve high accuracy and high velocity at the same time, with minimum overshoot and settling time, it could be used a control algorithm based on a two-phase movement of the end-effector [8]. Fig. 5 shows the valve control signal.

Fig. 6 shows the output position in time for a 125-mm-long trajectory experiment.

In the first phase, the motion is carried out with high velocity till the end-effector reaches 80% length of the trajectory. This phase is performed with a high gain proportional controller. The second phase is the approaching phase. It is carried out with a PI controller with small proportional gain [9]. The achieved results using experimental optimization were satisfactory, with a maximum steady state position error of 0.3 mm. The system is stabilized in less than 0.5 s.

In order to improve motion characteristics, the control algorithm can be divided in three phases. The first phase is the phase of high gains corresponding to high velocities. The second phase performs high deceleration. The final phase is the approximation phase at low velocity.

For distances to the goal more than 50 mm (high value of the position error), the control system uses a high value for the proportional gain. For position errors between 10 and 50 mm, a strong brake is used in order to allow the low velocity near the goal. For position errors less than 10 mm, a small value of gain

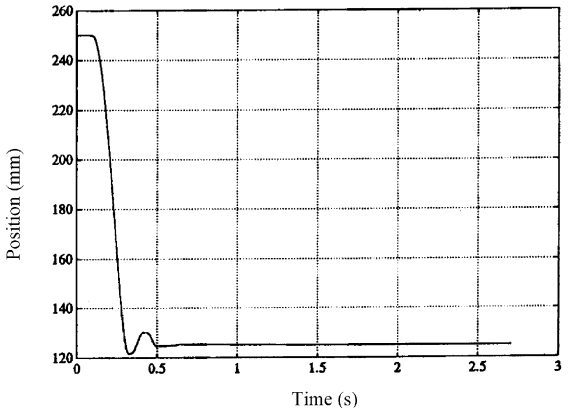

Fig. 6. Position versus time in seconds.

is used in order to avoid overshoot. During the brake phase, a velocity control is used. The braking signal is proportional to the velocity and the objective of this phase is to allow the low velocity near the goal. The velocity gains used in this phase depend on the velocity error.

System low natural frequency is a problem for high-speed operations. Air compressibility is a source of instability. The mathematical model is complex and it is difficult to obtain a suitable controller. A good approach to solve the problem is through the use of fuzzy control techniques.

The performance of the system is usually improved by the use of high proportional gains in the controller, but high proportional gains usually lead the system to instability. Control problems also arise from the system hysteresis and drift. When the cylinder is stopped there exists a range of output values that do not produce any movement of the cylinder during a given time period. This range of values is called *dead zone*. In order to start movement, an output signal to the valve is needed. Another source of instability arises from the fact of the valve hysteresis, defining a dead zone in its characteristic. Furthermore, system dead zone varies with time and cylinder position. The problem of valve hysteresis is solved, adding a 50-Hz component signal to the command [11]. In these conditions, the valve dead zone is negligible compared with the system dead zone.

When the cylinder is stopped, an output signal to the valve is needed in order to move the system. The lowest signal that moves the cylinder is defined as dead zone signal DZ. If the cylinder moves to the left and to the right, then DZl and DZr are the dead zone signals that make the left and the right movements. No movement is performed while the output signal $u(t)$ is between DZl and DZr, i.e., $\mathrm{DZl} < u(t) < \mathrm{DZr}$.

The dead zone signal is an output component signal designed to cancel the friction force. Its value depends on the movement direction: if the movement is to the right, DZr must be applied, otherwise DZl is applied.

When the cylinder is in motion, the static friction is neglected, so when the velocity is more than a certain value, the dead zone signal is applied to the opposite direction of the movement, i.e., if the cylinder moves to the right, DZl is applied, otherwise, DZr is applied.

The non-linear control algorithm can be described as follows:

- For absolute value of the position error more than 50 mm

$$u(k) = K_1 \mathrm{e}(k-1) + \mathrm{DZ},$$

where k is the discretised time and K_1 is a gain constant.

- If the absolute value of the position error is between 10 and 50 mm

$$u(k) = K_2 \mathrm{e}(k-1) + \mathrm{br}(k) + \mathrm{DZ},$$

where K_2 is another gain constant, and br(k) is a braking signal depending on the velocity and the position error. The objective of this signal is to slow down the cylinder near the goal in order to be positioned with precision and without overshoot.

- For absolute value of the position error less than 10 mm

$$u(k) = K_3 \mathrm{e}(k-1) + \mathrm{DZ},$$

where K_3 is another gain constant.

Fig. 7 shows the applied command signal and the position error for motion of the cylinder from 0 to 800 mm. The axis of the command and dead zone is in DAC (digital–analogue converter) units. The DAC used is a 12-bit DAC. The position error is defined as the difference between the desired position and the actual position, so the position error decreases from 800 to 0 in Fig. 7. The cylinder is positioned with an error less than 1 mm in 4 s.

Fig. 8 shows the applied command signal and the position error for motion of the cylinder from 800 to 30 mm. In this figure the position error is changed from -770 to 0 mm. The cylinder is positioned with an error less than 1 mm in 3.3 s.

3.3. Fuzzy control implementation

To control the positioning of the pneumatic manipulator, without developing the differential equations which govern the system behavior, it was implemented a Fuzzy Logic Controller. Using Matlab environment [12], C language routines were created to implement functions to be used in real-time communication and control. A graphical interface that contains the designed fuzzy logic controller was implemented.

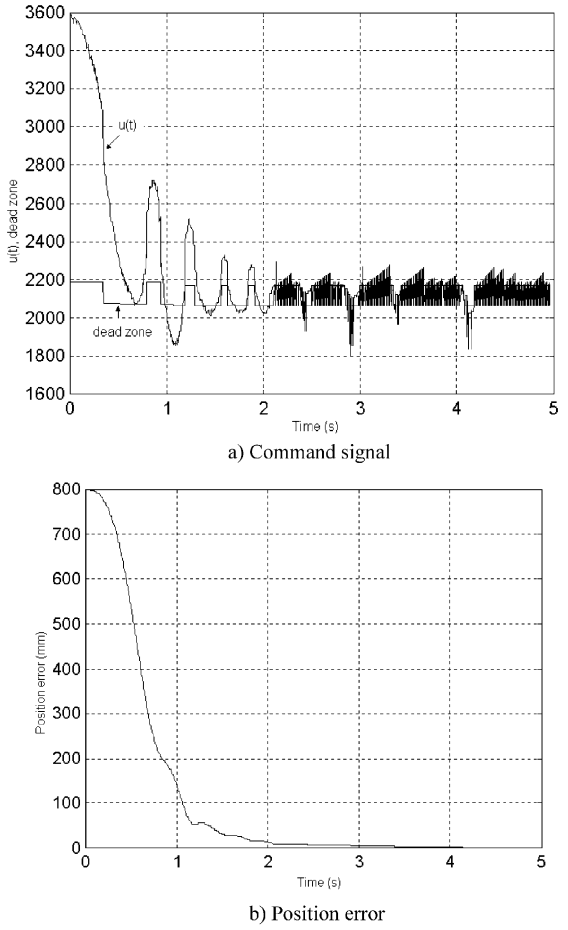

Fig. 7. Movement of the cylinder from 0 to 800 mm. (a) Command signal, (b) Position error.

System design consists in creation of the linguistic variables for the system, developing its structure, representing the information flow within the system, formulating the control strategy based on fuzzy logic rules and selecting the appropriate defuzzification method for this particular application.

A typical architecture for a Fuzzy Logic Controller can be viewed in Fig. 9.

The fuzzy controller is composed basically with four blocks: Fuzzifier, Knowledge Base, Inference and Defuzzifier [13]. The K_i parameters are multiplicative factors that establish a correspondence in the real values of the input and output variables and the universe of a discourse of these associated linguistic variables. The parameters allow defining of the variables in normalized universe of a discourse, like [0,1] or, the used $[-1,1]$. The K_i parameters are determined as:

$$K_i = 1/|E_{\mathrm{Mi}}|,$$

where $|E_{\mathrm{Mi}}|$ is the absolute difference between the biggest and the smallest values of the variables.

The position error (difference between the desired position and the actual position of the pneumatic cylinder) and the variation of the position error (difference between the current and the final position errors) were chosen as input variables. The command of the solenoid valve was chosen as output variable. The universe of discourse for the inputs has been normal-

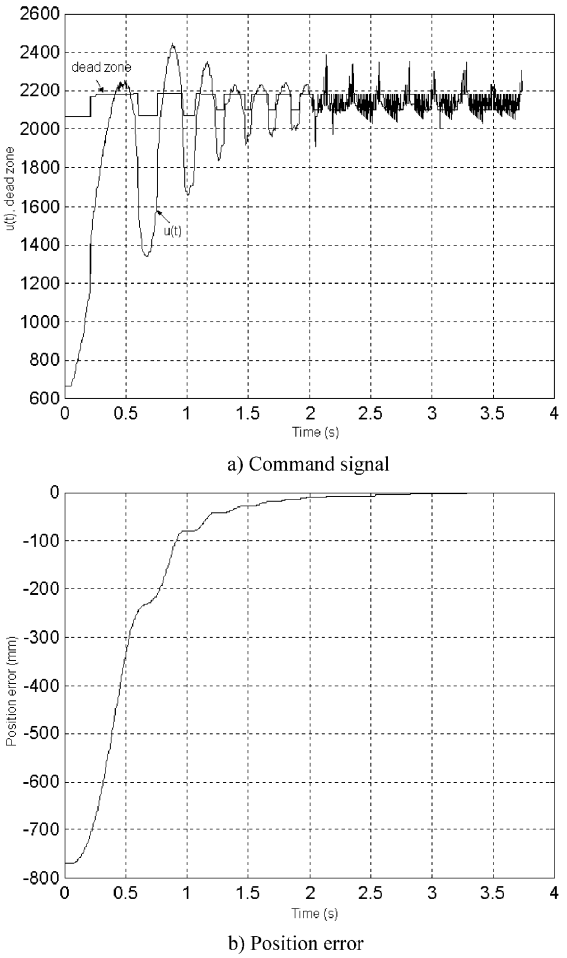

Fig. 8. Movement of the cylinder from 800 to 28 mm. (a) Command signal, (b) Position error.

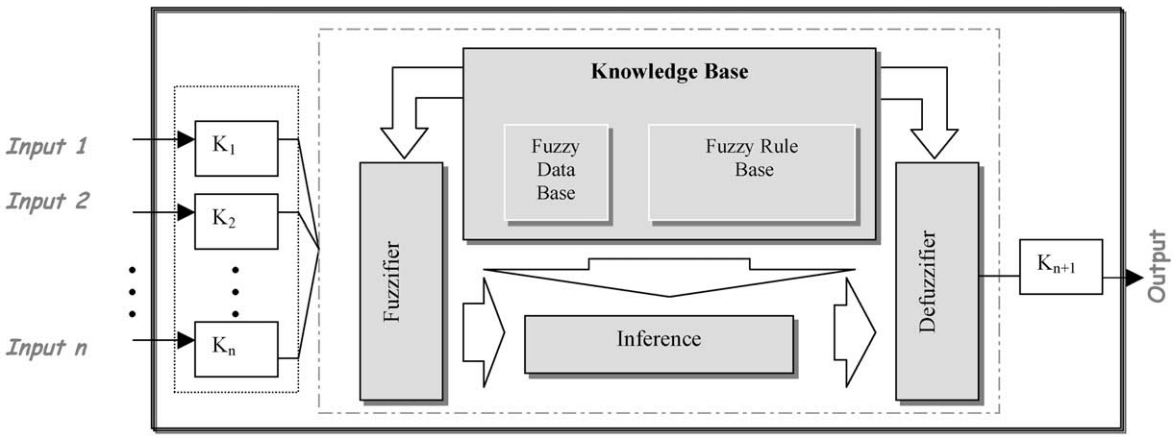

Fig. 9. Base architecture of a fuzzy logic controller.

ized due to the large number pulses from the incremental encoder.

To normalize the universes of the discourse for two inputs, $K_{\text{erropos}} = 1/|\text{erropos}|_{\max}$ and $K_{\text{varerropos}} = 1/|\text{varerropos}|_{\max}$ were used. The parameters $K_{\text{erropos}} = K_{\text{varerropos}} = 1/46{,}716 = 2.1406 \times 10^{-5}$, convert the universes to the range $[-1,1]$. The output variable has no normalized universe. The minimum and maximum values are 0 and 4096 (12 bits DAC). For the input variables, seven linguistic terms were used.

Most applications use between three and seven terms for each linguistic variable. One rarely uses fewer than three terms, since most concepts in human language consider at least two extremes and the middle between them. On the other hand, one rarely uses more than seven terms because humans interpret technical figures using their short-term memory. The human short-term memory can only compute up to seven symbols at a time [14].

Due to the fact that the system displacement behavior is symmetrical, the linguistic input variables have odd number of terms. Many different shapes of membership functions are proposed in scientific literature. However, using Matlab environment the selection should be more restrictive. Matlab membership functions include Standard Membership Functions: Triangular and Trapezoidal-type, Bell-type, Gauss-type and Sigmoid-type [12]. Standard MBF are only an approximation of the way how humans linguistically interpret real values. Psycholinguistic studies have shown that using the Spline membership functions the performance would be improved. The cubic Spline function (S-shape) are used to connect the points where the membership drops to zero.

For input variables erropos (position error) and varerropos (position error variation) the spline MBFs have Pi-type, S-type and Z-type. Figs. 10 and 11 show the MBF for input variables.

Fig. 12 shows the MBF for the output variable. Some rule labels in this picture are overlapped due to an automatic Matlab mode. The linguistic terms adopted for each membership function are Negative Large (NL), Negative Medium (NM), Negative Small (NS), Zero (ZR), Positive Small (PS), Positive Medium (PM) and Positive Large (PL).

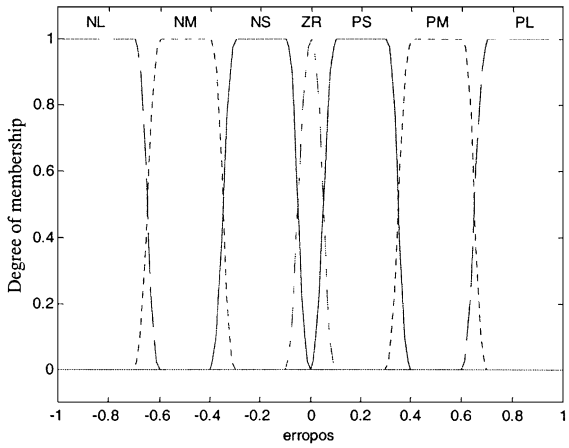

Fig. 10. MBF for input variable erropos.

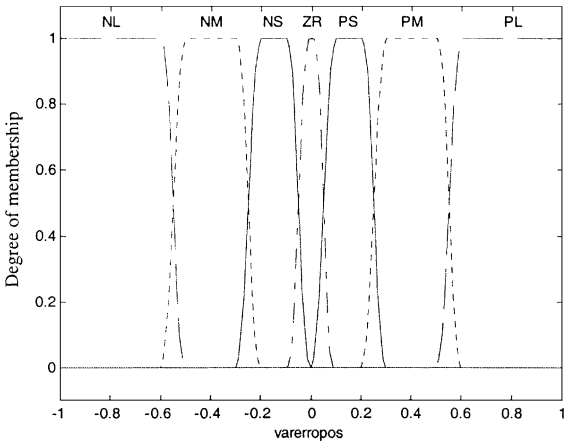

Fig. 11. MBF for input variable varerropos.

All that concerns the shape of membership functions deals only with membership function definitions for input variables of a fuzzy logic system. For output variables, most applications use only Λ-type (lambda or triangular) MBF. In this case for the rightmost and leftmost membership functions, a symmetrical *Z* and *S* membership functions are defined.

The rules of a fuzzy logic system represent the knowledge of the system. These rules were structured in blocks. For each combination of terms of the input variables, one rule is created with an "if" part (antecedent) and a "then" part (consequent). To combine the inputs in the antecedent, it was chosen the AND fuzzy logic operator. Initially, the degree of support for these rules was 1. The next step was the selection of the most plausible term for the consequent part of the rule, according to the knowledge acquired from the system past behavior. Fig. 13 shows the rule database.

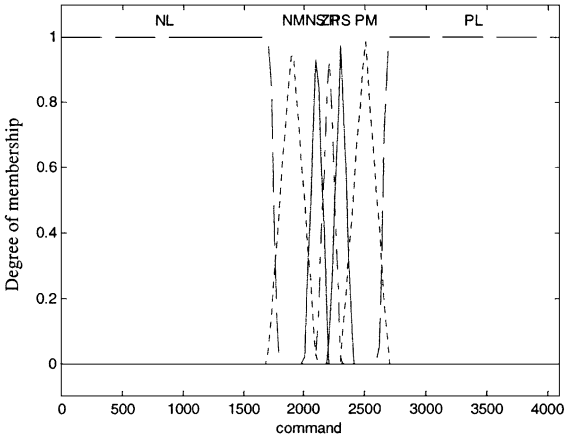

Fig. 12. MBF for output variable.

The method used for the implication from the antecedent to the consequent part was the *min operator*. The same method was used to connect the membership function in each antecedent rule.

The min operator of Mandani is defined as:

$$\mu_{A\to B}(u,v) = \mu_A(u) \wedge \mu_B(v).$$

To aggregate all outputs of each rule by joining their parallel threads, one of the tree-supported methods available by Matlab Fuzzy Logic Toolbox is used. The used method was the maximum method. The *max operator* is defined as:

$$\mu_{A\to B}(u,v) = \mu_A(u) \vee \mu_B(v).$$

The result of the fuzzy logic inference is the value of a linguistic variable. The conversion of such a linguistic result to an output value is the objective of the defuzzifier block.

Matlab environment has different methods of defuzzification. The most popular defuzzification method is the centroid calculation. This strategy has been shown to yield superior results [15]. Due to this reason, it was used. The centroid method is defined as:

$$z_{\mathrm{COA}} = \frac{\sum_{j=1}^{n} \mu_C(z_j) z_j}{\sum_{j=1}^{n} \mu_C(z_j)},$$

where n is the number of quantization levels of the output, z_j is the amount of control output at the

varerror / erropos	NL	NM	NS	ZR	PS	PM	PL
NL	NS	NM	NL	NL	NL	NM	NS
NM	ZR	NS	NM	NM	NM	NS	ZR
NS	PS	ZR	NS	NS	NS	ZR	PS
ZR	ZR	ZR	NS	ZR	PS	ZR	ZR
PS	NS	ZR	PS	PS	PS	ZR	NS
PM	ZR	PS	PM	PM	PM	PS	ZR
PL	PS	PM	PL	PL	PL	PM	PS

Fig. 13. Rule database.

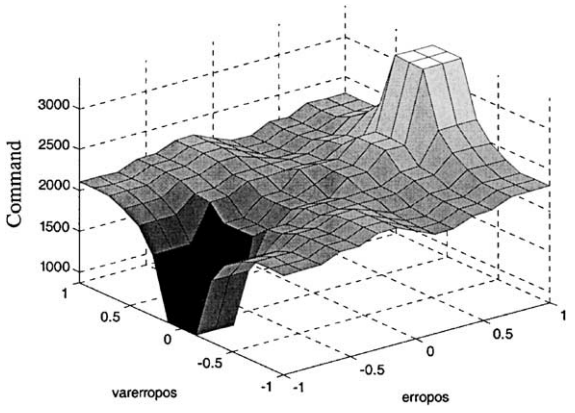

Fig. 14. FLC control surface.

quantization level j, and $\mu_C(z_j)$ represents its membership value in the output fuzzy set C. Fig. 14 shows the control surface of the FLC.

Some experimental results were conducted under the FLC. The position error of the cylinder while 100- to 560-mm positioning is shown in Fig. 15. Notice the evolution of the position error from 460 to 0 mm.

Compared to classical control, the performance of the FLC is quicker. Nevertheless, some oscillations were introduced. This may be improved by the better tuning of the rules.

Fig. 16 shows another test, when the cylinder goes from 0 to 1000 mm.

In this case, the response is quicker also but there exist some oscillations. To overcome this problem a

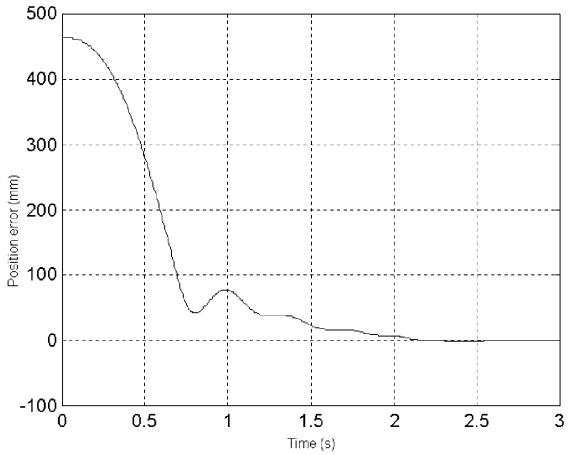

Fig. 15. Position error of 460-mm distance.

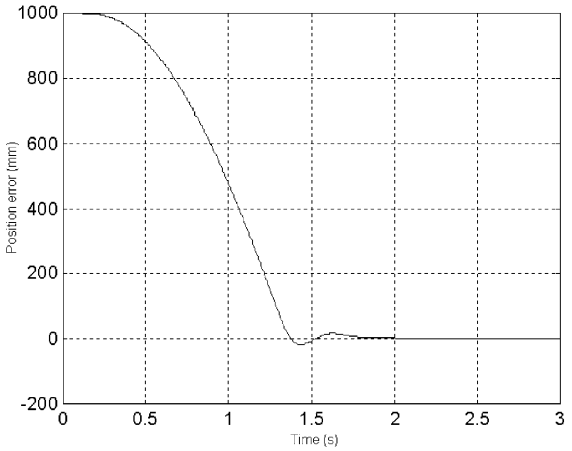

Fig. 16. Position error of 1000-mm distance.

fuzzy logic controller was implemented. Test results show that the implemented FLC is quicker than the implemented non-linear controller but has some oscillations, which can be acceptable in many construction tasks.

4. Conclusions

Problems of pneumatic manipulator positioning along angle trajectories and long linear trajectories were solved by means of theoretical, experimental and fuzzy logic approaches. The proposed techniques can be applied depending on the peculiarities of a given construction task.

The theoretical approach allows for optimizing the angle manipulator positioning control, for example of the industrial double-acting pneumatic manipulator "Tsiclon" [7], in the sense of flexibility and energy consumption for such tasks as welding and inspection inside pipes and other cylindrical surfaces. Further development can be done in optimizing three-dimensional positioning of a manipulator's end-effector.

The experimental approach simplifies a positioning controller structure for long linear trajectories of the manipulator end-effector. It gives a possibility to perform more reliable tasks such as transporting of construction elements to a working zone that changes in time. This result can be used in control systems of construction gantry type manipulators [16].

The simple implementation of the fuzzy controller, compared to classical methods, makes it more useful for construction applications. The design of the fuzzy controller increases the flexibility of applications, as it can be used in different manipulators or with the same manipulator with different payloads. Fuzzy design is based on rules that do not need an accurate mathematical description of the system. This advantage is important for applications where the system dynamics is changing in time or with a task, for example while polishing or performing another treatment of uneven construction surfaces.

Future development of the fuzzy logic technique should be done in the direction of using a combination with other intelligent control techniques, such as neural networks or genetic algorithms in order to adjust automatically the controller parameters.

References

[1] V. Gradetsky, M. Rachkov, Wall climbing robot and its application for building construction, Mechatronic Systems Engineering, vol. 1, Kluwer Academic Publishing, Dordrecht, 1990, pp. 225–231.

[2] Fr.-W. Bach, M. Rachkov, J. Seevers, M. Hahn, High tractive power wall-climbing robot, Autom. Constr., vol. 4 (3), Elsevier, Amsterdam, 1995, pp. 213–224.

[3] S. Kawamura, K. Miyata, H. Hanafusa, K. Ishida, PI-type hierarchical feedback control scheme for pneumatic robots, Proc. IEEE Int. Conf. On Robotics and Automation, Scottsdale, 1989, pp. 1853–1858.

[4] B.W. McDonnel, J.E. Bobrow, Adaptive tracking control of an air powered robot actuator, ASME J. Dyn. Syst., Meas., Control 1 (1993) 427–433.

[5] S.R. Pandian, Y. Hayakawa, Y. Kanazawa, Y. Kamoyama, S. Kawamura, Practical design of a sliding mode controller for pneumatic actuators, ASME J. Dyn. Syst., Meas. Control 119 (1997) 666–674.

[6] M. Rachkov, Optimal control of the transport robot, Proc. of the 20th Int. Conf. on Industrial Electronics Control and Instrumentation, (Bologna, Italy) vol. 2, 1994, pp. 1039–1042.

[7] M. Rachkov, Simulation of an observer for a control system of a pneumatic manipulator, Proc. of the Int. Conf. on Identification and Control of Systems, Moscow, 2000, pp. 115–121.

[8] Ya. N. Reutenberg, Automatic Control, Nauka, Moscow, 1978 (in Russian).

[9] M. Rachkov, L. Marques, A.T. de Almeida, Optimal control of pneumatic manipulators for construction application, Proc. of the 18th Int. Symp. on Automation and Robotics in Construction, Krakow, Poland, 2001, pp. 253–258.

[10] A.T. de Almeida, P. Menezes, H. Fachada, Servo-pneumatic manipulators for the plastics industry, Proc. of the First Int. Conference on Applications of Industrial Electronics Systems, 1990.

[11] J. Pu, R.H. Weston, Motion control of pneumatic drives, Microprocess. Microsyst. 12 (7) (1988) 373–382.

[12] J.S. Jang, N. Gulley, Fuzzy Logic Toolbox, The MathWorks Inc., Natick, MA, 1995.

[13] G. Lee, L. Chin-Teng, Neural Fuzzy Systems—A Neuro-Fuzzy Synergism to Intelligent Systems, Prentice-Hall, New York, 1996, ISBN 0-13-235169-2.

[14] C. Altrock, FuzzyLogic and NeuroFuzzy Applications Explained, Prentice-Hall, 1995, ISBN 0-13-368465-2.

[15] M. Braae, D.A. Rutherford, Fuzzy relations in a control setting, Kybernetes 7 (3) (1978) 185–188.

[16] TEGOPI SA, http://www.tegopi.pt.